Digital Terrain Model (DTM) from Indian Remote Sensing (IRS) Satellite Data from the Overlap Area of Two Adjacent Paths Using Digital Photogrammetric Techniques

T. Ch. Malleswara Rao, K. Venugopala Rao, A. Ravi Kumar, D. P. Rao, and B. L. Deekshatula

Abstract

Present day needs for medium- and small-scale topographic mapping at reduced cost and time can be met by using stereoscopic digital data acquired by present and planned satellites. In anticipation of the planned IRS-1C stereo data, attempts are made to use the overlap area between two adjacent paths of IRS-1A linear imaging self scanning (LISS)-II data as a stereo pair for generating a digital terrain model (DTM) using digital photogrammetric techniques. Software has been developed to recover the epipolar geometry of the stereo pair and to accomplish automated digital stereo matching to find the corresponding points in the left and right images by correlation techniques to calculate parallax to the sub-pixel level. The parallax is then used in conjunction with the IRS-1A data acquisition system to compute relative elevations. The absolute DTM is generated by referring the relative elevation to a few control points with known Z-coordinates. To evaluate the developed methodology and the software, three test sites at different locations in India near Palghat, Pune, and Dehradun were selected. It is observed that the overlap area between two adjacent paths increases from the equator to the poles whereas the base-to-height ratio (B/H) decreases. A methodology to calculate the percentage of overlap and B/H value at a given latitude is presented. The resultant DTMs for the three test sites were evaluated for error, and it is observed that 90 percent of RMSz errors fall within 33.95 m, 34.45 m, and 38.12 m at Palghat, Pune, and Dehradun, respectively. The DTM and the corresponding IRS-1A data are used to generate 3D perspective images. The software package developed will have potential usage in 3D analysis of IRS-1C stereo data.

Introduction

With the launch of the first Earth Resources Technology Satellite, now called Landsat-1, remote sensing gained international popularity. Digital data acquired with a wide series of sensors used onboard the Landsat series, SPOT, IRS-1A, and IRS-1B satellites proved to be an effective source of information to explore and monitor the Earth's dwindling resources and its environment. Topographic mapping, on the other hand, has not benefited greatly to date from the use of orbiting satellites owing to the poor geometry of the imagery acquired with remote sensing sensors. The great worldwide demand for topographic maps, mainly in the developing countries, requires the acquisition of metric stereo data from a space platform which would cover large areas at reasonably high speed with a reduction in the density of geodetic control.

The next decade will see new technological developments in this field with the launching of planned stereo mapping satellites, including the IRS-1C satellite of India during 1994-95 (Department of Space, 1989). At present, in the absence of metric stereo satellite data, the overlap area between two adjacent paths of existing IRS-1A or IRS-1B satellites may be used as stereo data for small-scale topographic mapping limited to the overlap area. The IRS-1A sensor payload system consists of two pushbroom LISS-II cameras of 36.25-m spatial resolution and one LISS-I camera of 72.5-m spatial resolution employing linear charge coupled device (CCD) arrays as detectors. Each camera system images in four spectral bands in the visible and near infrared regions (Department of Space, 1989). The reflected energy for each picture element sensed by the detector is quantized into 128 gray levels.

The main objective of this work was to develop the methodology and the software system to evaluate IRS-1A LISS-II data from the overlap area of two adjacent paths at different locations in India for generating a DTM. Steps for the generation of a DTM are shown in Figure 1.

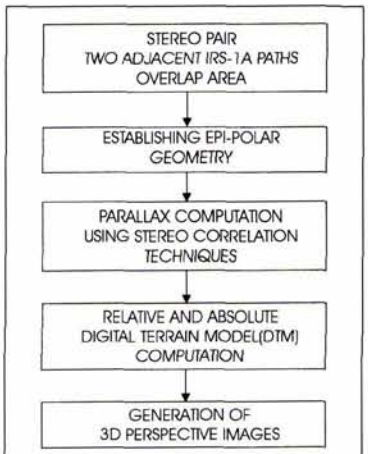

Figure 1. Steps for generation of DTM.

National Remote Sensing Agency, Hyderabad 500 037, India.

Photogrammetric Engineering & Remote Sensing, Vol. 62, No. 6, Month 1996, pp. 727–731.

0099-1112/96/6206-727$3.00/0
© 1996 American Society for Photogrammetry and Remote Sensing

Figure 2. Test sites locations.

Data Sets and the Study Area

To realize the objective of this work, three sets of IRS-1A LISS-II adjacent paths data of path-row 25-61 of 5 February 1989 and path-row 26-61 of 6 February 1989 (near Palghat, 10°N by 77°E), path-row 29-55 of 5 February 1991 and path-row 30-55 of 6 February 1991 (near Pune, 18°N by 74°E), and path-row 28-46 of 22 December 1990 and path-row 29-46 of 23 December 1990 (near Dehradun, 30°N by 78°E) were selected and acquired in band interleaved by line format. The locations of the above selected data sets are shown in Figure 2, and the Pune test area data are shown in Figure 3. Overlap area images of 512 by 512 pixels, 730 by 350 pixels, and 512 by 512 pixels were selected for generating DTMs at Palghat, Pune, and Dehradun, respectively.

Computation of Overlap Area and Corresponding B/H Value

IRS-1A is operating in a circular sun-synchronous near-polar orbit at an inclination of 99.02° and at an altitude of approximately 904 km. The distance between the adjacent orbits is maximum at equator and linearly decreases towards poles. As a result, IRS-1A LISS-II (combined) will have an adjacent paths overlap area of 10 percent at the equator and 32 percent at 40° latitude (Department of Space, 1989).

In this study, the following methodology has been developed to calculate the percentage of overlap and the *B/H* value between the two adjacent IRS-1A paths. The adjacent paths of the Pune test area are shown in Figure 4.

The distance between the two adjacent paths (B) can be obtained as

$$B = \mathrm{SW} - (\mathrm{SW} * \mathrm{OL}) \quad (1)$$

where SW is the IRS-1A swath width (148 km) and OL is the percentage of overlap area between two adjacent paths.

The percentage of overlap area between the two adjacent paths at a given latitude is computed as

$$\mathrm{OL} = 0.55 * d + 0.075 * m + 0.0125 * s + 10.0 \quad (2)$$

where d, m, and s are degrees, minutes, and seconds of a given latitude, respectively.

The number of overlap pixels can be computed as

$$\mathrm{NP} = (4096 * \mathrm{OL}) \quad (3)$$

As long as the roll error does not change between the two consecutive days, the above equations hold. The change in roll error may increase or decrease the overlap as explained below (Department of Space, 1989).

A reduction in overlap occurs when the roll error pulls the images apart. The maximum reduction in overlap is 12.7 km due to a maximum roll change, which occurs when roll is +0.4° on the Nth day and roll is −0.4° on the $(N+1)$th day. This is very rare.

An increase in overlap occurs when the roll error shifts the images closer. The maximum increase in overlap is 12.7 km due to a maximum roll change, which occurs when roll is −0.4° on the Nth day and roll is +0.4° on the $(N+1)$th day. This is also a very rare case.

The percentage of overlap and the *B/H* values for the three test study areas were computed and are presented in Table 1.

Orienting Digital Stereo Pairs

In the satellite stereo images, there are two types of parallax: vertical parallax (Y-parallax), due to spacecraft motion errors, and horizontal parallax (X-parallax), due to terrain relief, which is of interest for topographic mapping. Before finding X-parallax by automated techniques, it is necessary to align the two images along the horizontal axis; in other words, remove the Y-parallax so that parallax exists only in the horizontal direction. This is referred to as epipolar alignment, which helps in reducing the search area for matching corresponding image points. In order to achieve the epipolar geometry of a stereo pair, either a parametric or a non-parametric approach may be used. The parametric approach requires that all imaging parameters be available. In the present work, in order to establish the epipolar geometry of the stereo pair, a non-parametric method is used. A non-parametric method does not require the ancillary data that was recorded during image acquisition. This approach uses a mathematical function relating image coordinates and corresponding ground control points (GCPs). To ensure that both images of the stereo pair are mapped to one coordinate system, a set of GCPs of near equal elevation that appear in both the left and right images are collected, and their corresponding latitudes and longitudes are determined from 1:50,000-scale Survey of India (SOI) topographic maps. Both the images are then rectified to a common coordinate system using a first-order polynomial transformation. The withheld GCPs are used to evaluate the RMS planimetric error (RMSExy) values. RMSExy values were found to range from 10 m to 15 m.

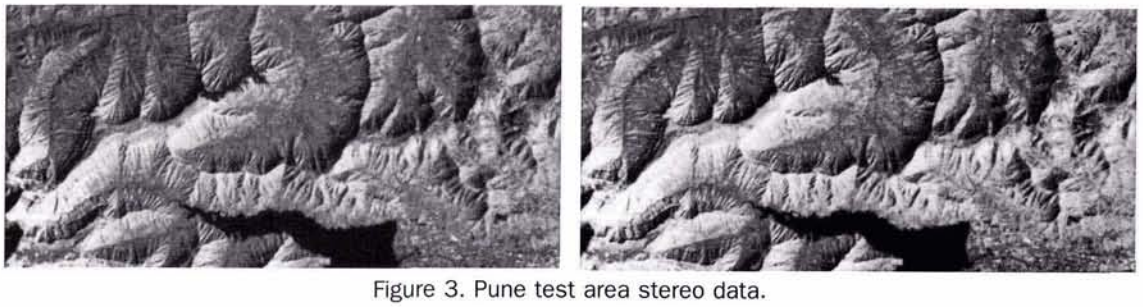
Figure 3. Pune test area stereo data.

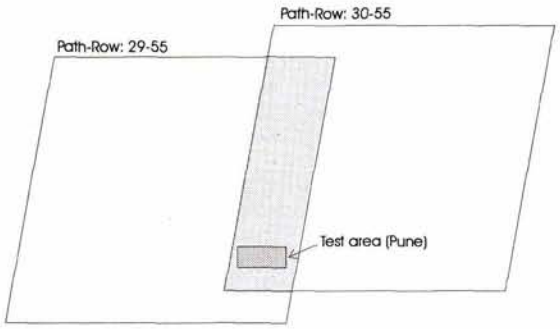

Figure 4. Adjacent paths overlap at Pune test area.

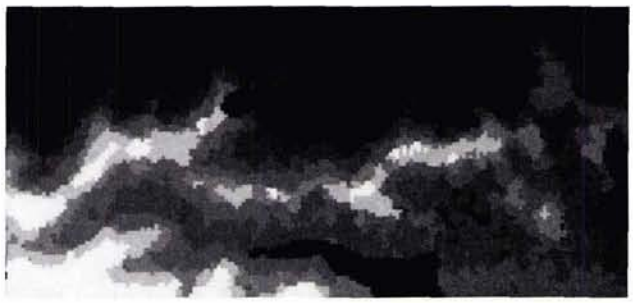
Figure 5. Pune area parallax gray level image.

Computation of Parallax Using Correlation Techniques

To determine the correspondence between the point of interest in the left image and its corresponding point in the right image, there are two approaches: feature-based matching and area-based matching. In feature-based matching, structural data (edges) are first extracted in each image separately, and matching criteria are then applied. Feature-based matching has not been very popular in photogrammetry. However, successful applications have been reported (for example, Forster (1986) and Hahn and Forstner (1988)). In area-based matching, the correspondence between the pairs of points is determined by evaluating the similarity of small areas around each pixel. Two techniques are used in area-based matching. The first technique is based on the use of a correlation function to determine a coefficient from which to decide whether a point in the left image corresponds to another in the right image. The second technique is based on an iterative least-squares resolution algorithm. Principles of least-squares matching have been published by Forstner (1982) and have been extended in a number of ways (Rosenholm, 1987; Wrobel, 1987; Helava, 1988). From the earlier studies, area-based matching has proven to give good results (Brockelbank and Tom, 1991), particularly with optical data sets. In this study, it is proposed to apply the first technique of area-based matching. The prerequisite for this area-based matching is the radiometrically normalized stereo pair.

In this study, the right image of each data set is radiometrically normalized with reference to its corresponding left image as follows (Malleswara Rao and Deekshatulu, 1983):

$$g'_n = g_n\sigma_l/\sigma_r + (m_l - m_n\,\sigma_l/\sigma_n) \qquad (4)$$

where g'_n is the normalized right image pixel gray value, g_n is the right image input pixel gray value, σ_l is the standard deviation of the entire left image, σ_n is the standard deviation of the entire right image, m_l is the mean value of the entire left image, and m_n is the mean value of the entire right image.

In area-based matching, to measure the similarity of a small area around the point of interest, a correlation coefficient is computed based on the cross correlation function. Then it is determined where the point in the left image corresponds to its corresponding point in the right image. This method is explained with the Figure 5. A target area of window size $M1$ by $N1$ centered on the pixel P of the left image is applied to find its correspondence in the right image search window. The search window size is suitably selected to ensure that the corresponding point of interest is included and that its size $M2$ by $N2$ is always larger than the target window. The correlation coefficient is computed from the most commonly used cross correlation function as given in Equation 5 (Rosenholm, 1985; Cappellini *et al.*, 1991) for every pixel (m,n) in the search window by matching the target window: i.e.,

$$r(m,n) = \frac{\sum_{M1}\sum_{N1}(g_t - u_t)(g_s - u_s)}{\{[\sum_{M1}\sum_{N1}(g_t - u_t)^2][\sum_{M1}\sum_{N1}(g_s - u_s)^2]\}^{1/2}} \qquad (5)$$

where $r(m,n)$ is the correlation coefficient; $M1$, $N1$ is the size of the window; g_t, g_s are the center pixel values of the target window and corresponding search subwindow, respectively; and u_t, u_s are the target window and corresponding search area subwindow mean value, respectively.

The correlation coefficient value ranges between 1 and -1; 1 indicates complete similarity, 0 indicates no similarity, and -1 indicates opposite similarity.

The pixel coordinates, say $P'(x,y)$, where the maximum correlation value occurs in the search window, are identified as the coordinates of the corresponding point of P. Then the parallax is computed from the algebraic difference of P' and P.

In the CCD scanning system, the same unit area on the ground may not be represented as one pixel in the left and right images. This means that one pixel area in the left image may be shared by one to eight pixels in the right image. Therefore, to identify the appropriate correspondence portion of point P in the right image, the already calculated 3 by 3 maximum correlation coefficients around the point P' are interpolated to calculate the sub-pixel parallax from Equation 6 (Gruen and Baltsavias, 1987): i.e.,

$$dx = \frac{r(x+1,y) - r(x-1,y)}{4r(x,y) - 2r(x+1,y) - 2r(x-1,y)} \qquad (6)$$

This sub-pixel parallax value (dx) is added to the earlier computed parallax value to get the total parallax at the point P. This method is applied to get the parallax at any point of interest in the image.

TABLE 1. PERCENTAGE OF OVERLAP AND B/H VALUES OF DATA SETS

Area name	Adjacent path-row	% of overlap area	B (kms)	H (kms)	B/H
Palghat	25-61 & 26-61	15.5	122.86	904	0.1359
Pune	29-55 & 30-55	19.9	117.74	904	0.1302
Dehradun	28-46 & 29-46	26.5	108.78	904	0.1203

Implementation

Band 4 data for the three test areas have been used for the computation of parallax. The above explained parallax computation method is implemented in three stages. In the first stage, the maximum correlation point is identified by moving

Plate 1. Palghat test area 3D perspective image.

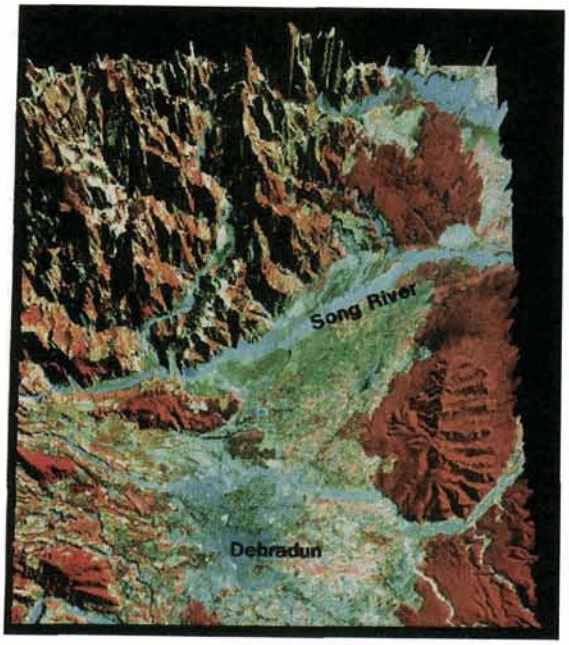

Plate 3. Dehradun test area 3D perspective image.

the 11 by 11 target window within the 21 by 13 search window, allowing a ± 1 pixel maximum deviation in the Y-direction and ± 5 pixels in the X-direction. In the second stage, the point of maximum correlation is modified by moving a 5 by 5 or 3 by 3 window within the 11 by 11 search window. Finally, the sub-pixel parallax value is interpolated using Equation 6, and the total parallax is computed.

Measuring the parallax at every point is neither efficient nor computationally economical (Ehlers amd Welch, 1987). Therefore, parallax is computed at a 3-pixel interval in both the X and Y directions. The obtained parallax file has been filtered to remove mismatches or noise using a conditional filter. The final parallax for all the image points is interpolated from the above computed parallax data using a cubic interpolation technique (Holkenbrink, 1978). The gray level parallax image of the Pune area is shown in Figure 6. The light areas represents high parallax values and the dark areas low parallax values. The obtained parallax is then used to compute the corresponding DTM, as described in the next section.

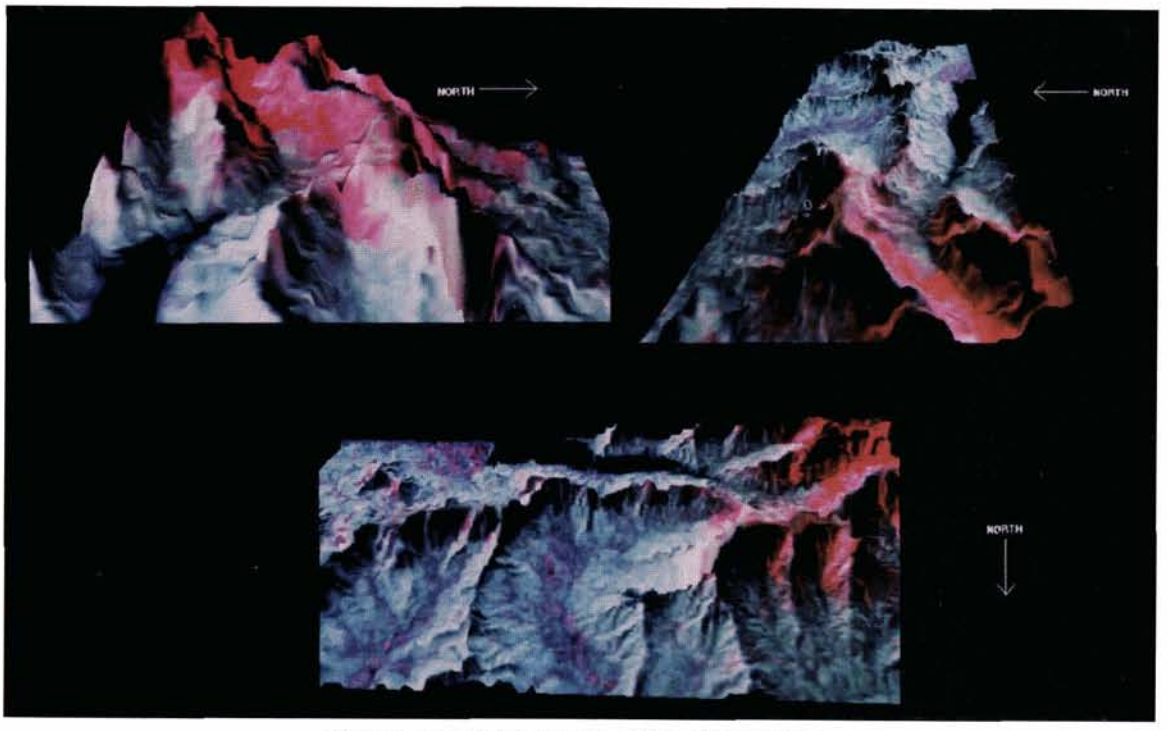

Plate 2. Pune test area 3D perspective images.

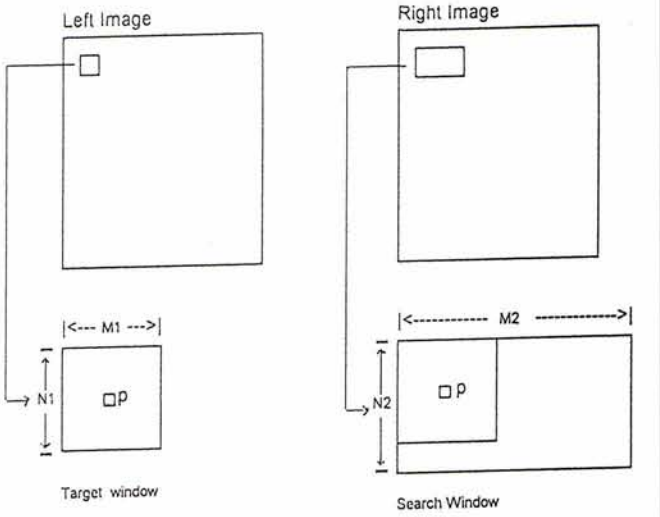

Figure 6. Two-dimensional matching principle. The correlation window (*M1* by *N1*) is moved over all possible locations within the search window (*M2* by *N2*). At each location, the correlation coefficient is computed.

Digital Terrain Model (DTM) Computation

A relative DTM can be computed from the parallax as follows (Ehlers and Welch, 1987):

$$dh(x,y) = dx(x,y)\ H/B \qquad (7)$$

where $dh(x,y)$ is the relative height at x,y: $dx(x,y)$ is the parallax at x,y; H is the satellite altitude; and B is the distance between adjacent paths.

The absolute DTM is created by scaling the relative DTM by linear regression techniques with 12 well distributed GCPs of known Z-coordinates collected from the SOI. The terrain elevation accuracies of the generated DTMs for the three test areas are checked at the 30 known test points. It was found that the RMSEz values are 33.95 m, 34.45 m, and 38.12 m at the Palghat, Pune, and Dehradun test areas, respectively. From the results, it is evident that the RMSEz increased from first data set to third data set, whereas the *B/H* value decreased. The resultant DTMs are used along with the corresponding IRS-1A data to generate the 3D perspective images. Plates 1, 2, and 3 show the 3D perspective images of the Palghat, Pune, and Dehradun areas, respectively.

Conclusions

The presented method and results have shown the ability to provide conceptual solutions for some basic problems in the use of the overlap area from two adjacent IRS-1A paths as stereo data for generating a DTM using digital photogrammetric techniques. In this study, the DTMs generated for three test sites have shown different RMSEz values because the *B/H* value is not same at these sites. In the case of IRS-1A, the elevation accuracies are high at the equator and decrease linearly towards the poles because the *B/H* value is maximum at the equator and minimum at the poles.

The resultant DTMs are sufficient for production of 3D perspective images, ortho images, small-scale (1:250,000 or smaller) GIS applications, and also for the interpolation of contours for small-scale topographic maps.

Because the performance of the proposed method has been tested with three data sets of IRS-1A LISS-II adjacent paths overlap areas at different locations in India, this work is a forerunner for preparing to process the future IRS-1C stereo data.

References

Brockelbank, D.C., and Ashley P. Tom, 1991. Stereo Elevation Determination Technique for SPOT Imagery, *Photogrammetric Engineering & Remote Sensing*, 57(8):1065–1073.

Cappellini, L., L. Alparone, G. Galli, P. Lange, A. Mecocci, and L. Menichetti, 1991. Digital Processing of Stereo Images and 3D Reconstruction Techniques, *International Journal of Remote Sensing*, 12(3):477–490.

Department of Space, Government of India, 1989. *Indian Remote Sensing Satellite Data Users Hand Book*.

Ehlers, M., and R. Welch, 1987. Stereocorrelation of Landsat TM Images, *Photogrammetric Engineering & Remote Sensing*, 53(9): 1231–1237.

Forstner, W., 1982. On the Geometric Precision of Digital Correlation, *International Archives for Photogrammetry and Remote Sensing*, 24(3):176–189.

———, 1986. A Feature Based Correspondence Algorithm for Image Matching, *International Archives for Photogrammetry and Remote Sensing*, 26(3/3):150–166.

Gruen, A.W., and E.P. Baltsavias, 1987. High Precision Image Matching for Digital Terrain Model Generation, *Photogrammetria*, 42(3):97–112.

Hahn, M., and W. Forstner, 1988. The Applicability of a Feature-Based and a Least-Squares Matching Algorithm for DEM-Acquisition, *International Archives for Photogrammetry and Remote Sensing*, 27(39):137–150.

Halava, U.V., 1988. Object-Space Least-Squares Correlation, *Photogrammetric Engineering & Remote Sensing*, 54(6):711–714.

Holkenbrink, P.F., 1978. *Manual on Characteristics of Landsat Computer-Compatible Tapes Produced by the EROS Data Center Digital Image Processing System*, Geological Survey, EROS Data Center, Sioux Falls, South Dakota, pp. 6–7.

Malleswara Rao, T.Ch., and B.L. Deekshatulu, 1983. Techniques for Minimizing Radiometric Striping Effects in Landsat Data, *Photonirvachak, Journal of Indian Society of Photo Interpretation and Remote Sensing*, 11(1):31–36.

Rosenholm, D., 1985. *Digital Matching of Simulated SPOT Images*, Fotogrammetriska Meddelanden, Department of Photogrammetry, Royal Institute of Technology, Stockholm.

———, 1987. Least-Square Matching Method: Some Experimental Results, *Photogrammetric Record*, 10:493–512

Wrobel, B., 1987. Facet Stereo Vision (FAST Vision) — A New Approach to Computer Stereo Vision and to Digital Photogrammetry, *Proceedings of Intercommission Conference on Fast Processing of Photogrammetric Data*, Interlaken, Switzerland, pp. 231–258.

To Participate in Your Local Region Activies ...

... Contact the ASPRS Membership Department 301-493-0290, ext. 29; fax: 301-493-0208; or email: members@asprs.org.